Advances in Engineering Research, volume 207
Proceedings of the 2nd International Seminar of Science and Applied Technology (ISSAT 2021)

Response of Cable-Stayed Bridge Under Ground Motions
A Case Study of Sei Dareh Cable-Stayed Bridge

Afdhal Lazuardiansyah Ramdhani[1,*] Riawan Gunadi[1]

[1] *Department of Civil Engineering Politeknik Negeri Bandung, Indonesia*
[*] *Corresponding author. Email: afdhal.lazuardiansyah.mtri19@polban.ac.id*

ABSTRACT
The cable-stayed bridges are vulnerable to vibrations caused by earthquakes. This study focuses on the Sei Dareh Cable-Stayed bridge that is at a relatively high level of vulnerability based on the 2017 Indonesia earthquake map. In this research, the study discussed the response of the Sei Dareh cable-stayed bridge under eleven ground motion accelerograms. The analysis was based on linear elastic conditions, so that it obtained the natural frequency, maximum displacement in the middle of the span and the top of the pylon, the stress of the cable and edge beam, and dynamic amplification factor (DAF). The three-dimensional finite element model (3D-FEM) of the bridge was established. Then, the model was analyzed under eleven ground motion accelerograms that have been scaled using the local design response spectra. The study reveals that the first and second mode of structure is a vertical translation with 0,71s and 0,49s periods respectively. TCU060 and Tabas accelerogram ground motions caused the largest cable forces and stress contrary to the Imperial ground motions. The analysis results under eleven ground motions show that the top pylon and deck mid-span satisfy the PTI code allowable displacements. The dynamic amplification factor (DAF) is under 2,0 as the limit value.

Keywords: *Cable-stayed bridge, earthquake, accelerogram, 3D FEM, linear-elastic.*

1. INTRODUCTION

There were two types of cable bridge namely a suspension bridge and a cable-stayed bridge. A cable-stayed bridge is a structure with several points in each span between the towers supported upward in a slanting direction with inclined cables and consists of the main tower(s), cable-stays, and main girders [1]. The advantages of cable bridges are effective for long spans compared to other types of bridges, have economical construction costs, have relatively beautiful structural aesthetics, have has a lightweight structure [2]. However, every advantage has consequences that must be accepted. One of them is that the lightweight of the structure makes this bridge vulnerable to vibrations caused by dynamic loads due to wind and earthquake loads [3]. Moreover, Indonesia was in an area that is prone to earthquakes because of its geographical location close to the three active tectonic plates of the world, namely Indo-Australia, Eurasia, and the Pacific (Indonesian Agency of Meteorology, Climatology, and Geophysics). This causes the structure of buildings and bridges located in earthquake-prone areas to be considered against the impact of the damage.

The case study takes place in the Sei Dareh Bridge in West Sumatra. The Sei Dareh Cable-stayed Bridge is a new bridge built next to the existing bridge which is intended to unravel the congestion of road traffic. The bridge that connects two riversides of Batang Hari River has 123 meters long, 9 meters wide, and the pylon is 41 meters high.

Referring to the 2017 earthquake map, the bridge has a relatively high level of vulnerability. Although at the design stage the bridge has been calculated against earthquake loads with response spectra, SNI 2833: 2016 states that for bridges with important categories, time history must be considered [4]. Even the SNI 1726:2019 requires that it be calculated with eleven accelerograms ground motion recording data [5].

The study will discuss the response of the Sei Dareh cable-stayed bridge under eleven accelerogram ground motions. The scope of the analysis method is in linear

elastic condition so that it will be obtained the natural frequency, maximum displacement in the middle of the span and the top of the pylon, maximum reaction, capacity ratio, and stress cable stress of the longest cable.

2. LITERATURE REVIEW

Studies in the response of cable-stayed bridges under strong ground motion have been initiated since the early 1990s. The previous research relates to the response of cable-stayed bridges under strong ground motions will be only mentioned here. To observe the behavior of the cable-stayed bridge, the 3-dimensional finite element model was established [6]. This paper shows a detailed description of the development of one class of linear elastic finite element models for the dynamic analysis of a cable-stayed bridge. In a companion paper, the modal behavior predicted by the finite element model is compared to measured ambient vibration properties of the full-scale structure. Accelerogram ground motion spatial variability in the lateral x and y-direction was applied to the 3D FEM. The studies show that that multiple support seismic excitation can have a significant effect on the response displacements and member forces of such long and complex 3D FEM model structures [7]. The analysis method to observe the response can be reached with a nonlinear analysis that means until plastic condition, or just linear analysis so the structure was analysis on elastic condition like discussed [8]. The present study investigates the response of long-span cable-stayed bridge through the plane finite element model under three strong earthquake records (Kobe, Takatori, and Higashi) and applied as longitudinal, vertical, and combine longitudinal-vertical direction. To assess the seismic response of residual elastic-plastic, a new type of seismic damage index well-known as the maximum equivalent plastic strain ratio is suggested. Finally, the research reveals that the elastic-plastic effect leans to reduce the seismic response of long-span cable-stayed steel bridges. The elastic and elastic-plastic seismic response behavior depends highly on the characteristics of input earthquake records.

The application of longitudinal accelerogram records was commonly used to analyze the response of a high-rise building, but for cable-stayed bridges, vertical accelerogram records need to be considered. Previous similar research must be done by [9] and [10]. The study provides an analytical investigation on the influence of the near-fault vertical ground motions on the seismic behavior of the Karnali cable-stayed bridge. The behavior of the bridge subjected to ground motions with and without vertical accelerogram records was conducted using near-fault ground motions on a three-dimensional bridge model. The research reveals that the influence of vertical motion on the seismic response of the Karnali Bridge was few and coinciding peak vertical motion with peak horizontal motion also has fewer effects compared to the motion without such coincidence.

The studies about this not only carried out for the highway cable-stayed bridge but also to railway cable-stayed bridge [11]. In this research, a time-domain analysis framework for the train-bridge system subjected to accelerogram ground motion was carried out. The research simulates that the seismic ground motions have an important role in the dynamic response of the railway vehicles running on the long-span cable-stayed bridge under various spectrum characteristics, incident angles, occurrences times, and occurrence probabilities.

2.1 Elastic Linear

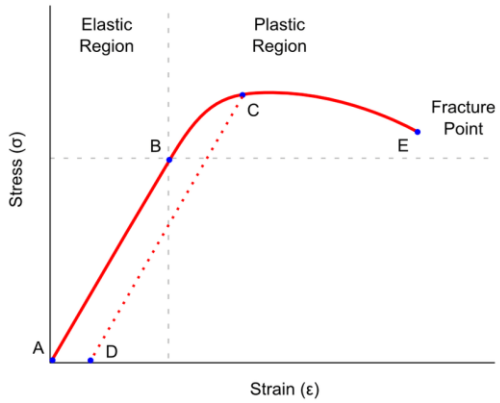

Figure 1 Stress-Strain Diagram

Figure 1 is a stress-strain relationship diagram of a material. In the figure, there are two regions, namely the elastic region (A-B) and the plastic region (B-E). In this study, the analysis was carried out only on the elastic condition, which means that the 3D analysis carried out on the structural model covers the capacity ratio check.

However, a long-span cable-stayed bridge exhibits nonlinear characteristics under any load level [8]. These nonlinear sources may come from the sag effect of inclined cable stays the combined axial load and bending moment interaction effect of the girder and tower, the large displacement effect, and the nonlinear stress train behavior of materials (material nonlinearity).

2.2 Time History Analysis

In the case of time history analysis of 3D structures with earthquake loads, the following equation (1) is used. [m], [c], [k] are the mass, damping and stiffness matrices, respectively. While $\ddot{u}$, $\dot{u}$, and u are acceleration, velocity, and displacement. Vector {r} is used to adjust the earthquake direction review according to applicable standards. For example, if the variances 1, 2, and 3 are translations towards the X-axis, respectively, translations towards the Y-axis, and rotations about the Z-axis.

$$[m]\{\ddot{u}\} + [c]\{\dot{u}\} + [k]\{u\} = -[m]\{r\}\ddot{x}_g \quad (1)$$

2.3 Scaling of Accelerogram Ground Motion

Accelerogram data is used as input to perform dynamic analysis of earthquakes with time history analysis. Time history analysis performed on a bridge structure may use actual spectral data obtained from accelerogram data for each period (unscaled). However, the earthquake data used in the analysis was taken from a different location from the bridge location being analyzed so that the seismic conditions may be different. Therefore, it is necessary to adjust the magnitude of the acceleration value in the original spectral data with the ground acceleration value at the location to be reviewed as a reference (target spectra).

Adjustment of the acceleration value is done by referring to the equation (2) written by [12] as follows:

$$SF = \frac{\sum_{TA}^{TB}(S_{a,target})^2}{\sum_{TA}^{TB}(S_{a,actual} \times S_{a,target})} \quad (2)$$

TA and TB are the limits of the vibration period range used in the calculation with the respective values for TA and TB 0.2T1 and 1.5T1 respectively [12]. T1 is the natural period of the structure of one degree of freedom under consideration.

2.4 Dynamic Amplification Factor

To quantify the effect of eleven accelerogram ground motions on the response of the cable-stayed bridge, dynamic amplification factor (DAF) which is the ratio between the dynamic response and the static response is carried out [13]. This result can be in the form of stress or strain. When using stress, the result being compared is internal forces, while when using strain, the result being compared is displacement.

3. METHODOLOGY

3.1 Structure Model

Based on Figure 2, the scope of the 3D model is just on the upper structure and pile cap while the bored pile is not modeled. The upper structural components consist of the deck structure, pylons, cables, and slabs. The deck structure consists of steel box elements, cross girders, and stringers are modeled in the software as “Beam” elements so that these elements can experience bending, shear, and axial forces, likewise on the pylon model. Meanwhile, the cable component is modeled as a “truss” element so that the element can only encounter axial tension and the initial tension force of the cable can be adjusted. The slabs were modeled as “thin-shell” without auto-meshing. So that, the model has 2773 nodes, 4290 beam elements, 24 truss elements, and 1800 shell elements. The boundary condition of the model consists of support (node 1, 2, 3, 4, 5, and 6) and link (node 7 and 8). Each node of support and link have their degree of freedom as shown on Table 1. Number 1 shows that the degree of freedom in this direction is restrained, while number 0 was released.

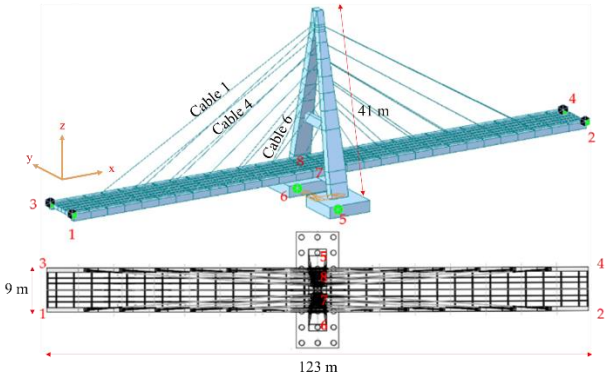

Figure 2 Finite element model and boundary condition

Table 1. Boundary condition of the 3D model

Node/ DOF	Dx	Dy	Dz	Rx	Ry	Rz
1	0	1	1	0	0	0
2	0	1	1	0	0	0
3	0	0	1	0	0	0
4	0	0	1	0	0	0
5	1	1	1	1	1	1
6	1	1	1	1	1	1
7*	0	1	1	0	0	0
8*	0	0	1	0	0	0

3.2 Scaling of The Accelerogram

Time history analysis begins with determining the response spectrum data for the Sei Dareh bridge based on SNI 2833:2016 as shown in Figure 3. The color of the red, blue, green, and yellow lines referred to soft soil (SE), rock (SB), medium soil (SD), and soft rock (SC). In this study medium soil (SD) is used as site class as target spectra. Then, continue by selecting the ground motion accelerograms which have the characteristics like the response spectrum of the Sei Dareh bridge area. Furthermore, the ground motion accelerograms scaling is for the Sei Dareh bridge area with the following scaling stages:

1. Change the actual ground acceleration data into actual response spectra (unscaled) according to the time history analysis procedure.
2. Calculate the value of the scale factor (SF) between the response of the target spectrum and the actual response spectrum in the period range between 0.2T to 1.5T calculated by equation (2).

3. Perform the process of scaling the actual ground acceleration data multiplied by the value of the scale factor (SF) to obtain the scaled ground acceleration. So, the following is the acceleration of ground motion used in this study as shown in Table 2.

Table 2. Ground motion records in analysis

No	Name	Station	Year	Magnitude
1	Imperial Valley	El Centro Array #7	1979	6,5
2	Superstition Hills	Parachute Test Site	1987	6,5
3	Loma Prieta	LGPC	1989	6,9
4	Erzincan Turkey	Erzincan	1992	6,7
5	Nortridge	Newhall-W Pico Canyon Rd	1994	6,7
6	Kobe, Japan	Port Island	1995	6,9
7	Duzce, Turkey	Duzce	1999	7,2
8	Kocael, Turkey	Yarimca	1994	7,4
9	Chi-Chi, Taiwan	TCU102	1999	7,8
10	Tabas, Iran	Tabas	1978	7,4
11	Chi-Chi, Taiwan	TCU065	1999	7,6

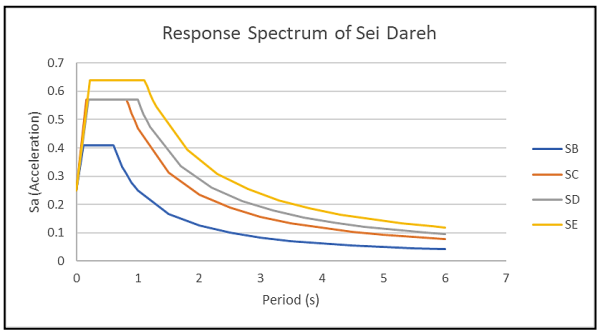

Figure 3 Spectra on bridge location

4. RESULT

Based on the linear analysis that has been carried out, the results are the mode shapes, mass participation ratio, cable force and tension, peak displacement of the beam in the half span of the bridge and pylon, and stress on the edge beam due to eleven accelerogram ground motion.

a. Mode shape

The mode shape shows the level of flexibility of the structure to vibrate. The smaller frequency makes the smaller stiffness structure so that it will vibrate easily. The first and second mode shapes are a vertical translation of the deck with 0,78s and 0,49s period respectively, while the third, fourth, and fifth mode shapes are deck rotations about the x-axis with 0,42s; 0,38s, and 0,31s period respectively. The mode shape of the structure is shown in the following Figure 4.

To fulfill a requirement for mass participation factor more than 90%, the mode shape in ritz-vector set up until 300 modes. Mass participation shows the contribution of the mass of the structure that vibrates when a vibration occurs, for example, due to an earthquake. Based on the analysis result, more than 90% mass participation is achieved at the 33rd mode for the x-direction, the 98th mode for the y-direction and, the 188th mode for the rotational-z.

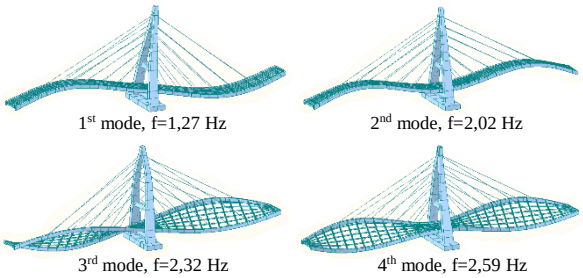

Figure 4 Mode shape of Sei Dareh Bridge's model

b. Force and stress cable

There are three cables evaluated related to its force, namely cable 6 which is located farthest from the pylon, cable 4 which is in the middle of the span of the bridge, and cable 1 which is closest to the pylon Figure 2. From Figure 5, each ground motion has a different duration of vibration and influences the cable force. It shows that the ground motion of TCU060 and Tabas has the most dominant influence among other ground motions. Meanwhile, Imperial ground motion has a relatively small effect on the resulting cable force. In addition, Figure 5 also shows that Cable 1 has a greater cable force than Cable 4 and 6. This is due to the different final pretension forces of the cable to form the chambers on the deck.

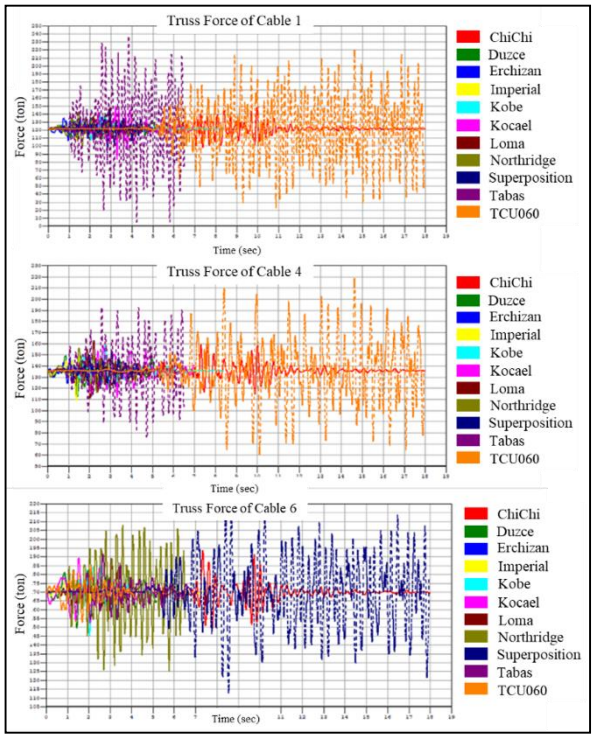

Figure 5 Truss Force of Cable 1, 4 and 6

The linear elastic analysis is carried out in this study so that the stress that occurs in the cable does not exceed the allowable stress. The allowable stress based on PTI is set at 45% of the tensile strength. If the cable has a tensile strength of 1860 MPa so the allowable stress is 837 MPa. Meanwhile, the cable stress caused by the eleven ground motions all meets the allowable stress as shown in Table 3.

Table 3. Stress of cable 1, 4, and 6 under eleven ground motions

Ground Motions		Stress Cable (MPa)		
Name	Station	C-1	C-4	C-6
ChiChi, Taiwan	TCU060	312.2	265.6	166.9
Loma Prieta	LGPC	84.2	87.5	58.1
Kocael, Turkey	Yarimca	90.9	72.6	80.6
Imperial Valley	El Centro Array #7	43.3	39.4	40.8
Tabas, Iran	Tabas	364.4	180.7	141.2
Superstition Hill	Parachute Test Site	77.0	55.7	71.1
Northridge	Newhall-Wpico Canyon	66.6	66.8	73.2
Kobe, Japan	Port Island	57.3	74.2	71.1
ChiChi, Taiwan	TCU102	86.0	79.9	88.4
Erzincan Turkey	Erzincan	48.1	52.2	52.9
Duzce, Turkey	Duzce	63.8	47.4	46.6

c. Displacement

According to the Post Tensioning Institute (PTI), the structural elements of the cable-stayed bridge that are most easily displaced are the top pylon and the edge beam at half span as shown in Figure 6. Based on the analysis, the ground motion that causes the largest longitudinal and transverse displacement on the top of pylon is Superstition of 7 mm and Tabas of 42.50 mm, respectively. Meanwhile, Duzce's ground motion provides a small displacement in both directions of displacement. Based on Figure 5, it can also be seen that the stiffness of the pylon in the transverse direction is greater than the longitudinal direction.

The largest vertical displacement on the deck is 28.70 mm under Tabas ground motion, while the largest horizontal displacement is 17.00 mm under Erchizan's ground motion. PTI provides that the displacement requirement for the Pylon is $\ell/300$, so if the pylon has a height of 41 meters, the allowable displacement is 136 mm. Meanwhile, the displacement requirement that occurs in the beam is $\ell/800$ so that the allowable displacement is 76,37 mm. Therefore, the displacement that occurs due to the eleven ground motions still meets the allowable requirements.

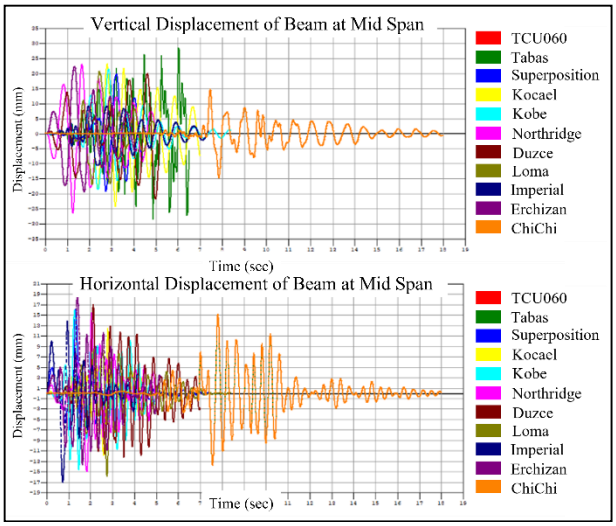

(a)

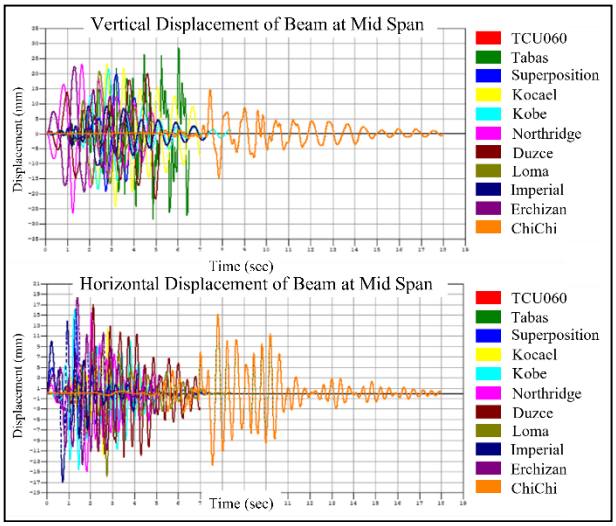

(b)

Figure 6 Displacement on (a) top pylon and (b) edge beam at mid-span

d. The stress of edge beam

The allowable stress for the edge beam is set at 45% of its tensile stress. If the edge beam has 490 MPa tensile strength, the allowable stress is 220,5 MPa. Edge beam under cables 1, 4 and, 6 are observed for the stress which is combined by bending about the y-axis and axial. Based on the analysis, TCU060 and Tabas ground motions gave the greatest stress to the edge beam on ½ (45 MPa), while the Imperial was on the contrary. So, based on the overall result, the stress on the edge beam under eleven ground motions are satisfy the requirement of allowable stress.

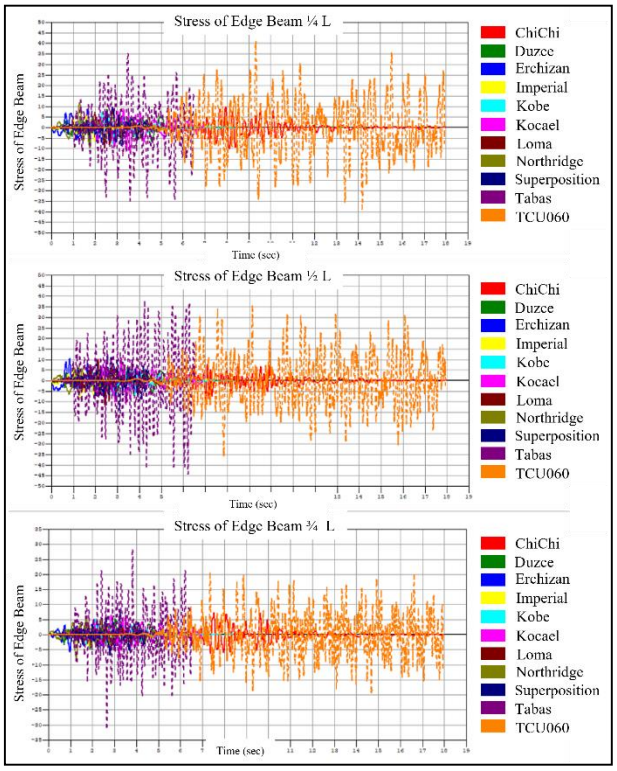

Figure 7 Stress of Edge Beam

e. Dynamic Amplification Factor (DAF)

As previously explained, DAF is calculated based on dynamic and static responses. In this study, static and dynamic responses were obtained from the internal forces in the stay cable (axial) and the edge beam (bending moment). The static response is obtained under gravity load, while the dynamic response is obtained under maximum responses to the eleven ground motions.

Based on the analysis, Table 4 shows that the highest DAF was obtained due to TCU060 and Tabas ground motions, namely 1.71, while the lowest was 0,80 due to Imperial ground motions. Teran et al., [13] revealed that in cable-stayed structures dynamic amplification factors caused by the sudden breakage of cables can be larger than 2.0. This fact is extremely important since design guidelines for cable-stayed bridges indicate that the highest value for such factors is 2.0 whereas under certain circumstances that value could be considered unsafe. Since all value of the amplification factor is under 2.0, so the structure is under a safe condition.

But this is different from the amplification factor obtained from the edge beams. Table 5 shows the highest DAF was obtained under TCU060 and Tabas with a value of 2.60 while the lowest was 1,90 due to Imperial ground motion This analysis shows that the structural responses under Tabas and TCU060 earthquakes exceed the DAF allowable value.

Table 4. DAF of stay cable under eleven ground motions

Accelerogram Ground Motions		Cable No		
Name	**Station**	**1**	**4**	**6**
ChiChi, Taiwan	TCU060	1.29	1.60	1.71
Loma Prieta	LGPC	1.39	1.41	1.71
Kocael, Turkey	Yarimca	0.86	1.12	1.56
Imperial Valley	El Centro Array #7	0.84	1.15	1.56
Tabas, Iran	Tabas	0.87	1.19	1.53
Superstition Hill	Parachute Test Site	0.89	1.16	1.58
Northridge	Newhall – W. Pico Canyon	0.82	1.16	1.49
Kobe, Japan	Port Island	0.80	1.08	1.49
ChiChi, Taiwan	TCU102	0.81	1.11	1.52
Erzincan Turkey	Erchizan	0.84	1.10	1.50
Duzce, Turkey	Duzce	0.88	1.18	1.60

Table 5. DAF of edge beam under eleven ground motions

Accelerogram Ground Motions		Edge Beam Close to Cable		
Name	**Station**	**1**	**4**	**6**
ChiChi, Taiwan	TCU060	2.37	2.03	2.47
Loma Prieta	LGPC	2.27	2.50	2.60
Kocael, Turkey	Yarimca	1.50	1.30	1.29
Imperial Valley	El Centro Array #7	1.61	1.52	1.44
Tabas, Iran	Tabas	1.32	1.38	1.29
Superstition Hill	Parachut e Test Site	1.43	1.34	1.57
Northridge	Newhall – W. Pico Canyon	1.28	1.28	1.24
Kobe, Japan	Port Island	1.26	1.26	1.19
ChiChi, Taiwan	TCU102	1.40	1.38	1.31
Erzincan Turkey	Erzincan	1.45	1.42	1.30
Duzce, Turkey	Duzce	1.38	1.45	1.36

5. CONCLUSION

This linear elastic analysis presents the response of The Sei Dareh Cable-stayed bridge under eleven ground motions. Based on the analysis result, the following conclusions are described:

1. The first and second modes of the structure are vertical translations with 0,78s and 0,49s period respectively, while the third, fourth, and fifth modes are rotations about the x-axis with 0,41s; 0,38s; and 0,31s period respectively.
2. TCU060 and Tabas accelerogram ground motions caused the largest cable forces and stresses, contrary to the Imperial ground motions that caused the lowest cable forces and stresses.
3. The analysis results under eleven ground motions show that the top pylon and deck mid-span satisfy the PTI code allowable displacements.
4. The test analysis results under eleven ground motions show that the edge beams closed to cables 1, 4, and 6 satisfy the allowable stress (45% of tension strength).
5. Based on the axial forces of the cables, the dynamic amplification factors (DAF) are under 2.0 as a limit value but based on the bending moments, the factors exceed 2.0.

AUTHORS' CONTRIBUTIONS

This work is led by Ramdhani as he modeled, analyzed, and wrote the manuscript of the full paper. Gunadi directed the method and evaluated the result of the analysis.

ACKNOWLEDGMENTS

This work was supported by the Tujuh Pilar Hijau consultant company and organized by the Ministry of Housing and Public Work.

REFERENCES

[1] L. Weiwei, Y. Teruhiko, Bridge engineering, Elsevier, 2017.

[2] T. Subramani, J. K. Rajan, V. R. Perumal, A. Palani, P. Kesavan, Design and analysis of suspension bridge, International Journal of Application or Innovation in Engineering & Manegemen (IJAIEM), vol. 8, 2019, pp. 83-91.

[3] N. Gupta, T. Barik, S. Dey, P. Effect of wind and seismic forces on different components of cable suspension bridge : An overview, Proceedings of National Conference on Advances in Structural Technologies (CoAST), 2019, pp. eleven-19

[4] Badan Standarisasi Nasional, SNI 2833 : 2016 Perencanaan jembatan terhadap beban gempa, 2016.

[5] Badan Standarisasi Nasional, SNI 1726 : 2019 Persyaratan beton struktural untuk bangunan gedung, 2019.

[6] J. C. Wilson, W. Gravelle, Modelling of a cable-stayed bridge for dynamic analysis, Earthquake Engineering and Structural Dynamics, vol. 20, 1991, pp. 707-721.

[7] A. S. Nazmy, A. M. A. Ghaffar, Effects of ground motion spatial variability on the response of cable-stayed bridges, Earthquake Engineering and Structural Dynamics, vol. 21, 1992, pp. 1-20

[8] W. X. Ren, M. Obata, Elastic-elastic seismic behaviour of long span cable-stayed bridges, Journal of Brdige Engineering, 1999, pp. 194-203

[9] B. Shrestha, R. Tuladhar, The response of Karnali Bridge, Nepal to near-fault eartquakes, Bridge Engineering, vol. 165, 2012, pp. 223-231

[10] B. Shrestha, Seismic response of long span cable-stayed bridge to near-fault vertical ground motions, KSCE Journal of Civil Engineering, Springer, 2014, pp.1-8, DOI : 10.1007/s12205-014-0214-y

[11] Y. Li, S. Zhu, C. S. Cai, C. Yang, S. Qiang, Dynamic response of railway vehicles running on long-span cable-stayed bridge under uniform seismic excitations. International Journal of Structural Stability and Dynamics, 2016, pp. 1-25, DOI : 10.eleven42/S0219455415500054

[12] E. Kalkan, A.K Chopra, 2010, Practical guidelines to select and scale earthquake records for nonlinear response history analysis of structures: U.S. Geological Survey Open-File Report 2010-1068, 124 p.

[13] Masrilayanti, P. B. Tarigan, R. Kurniawan, R. Aryanti, 2018, Kajian dynamic amplification factor (DAF) pada jembatan cable-stayed akibat beban gempa. 5th ACE Conference, 586-593 p.

[14] R. Teran, A.C Aparicio, 2007, Dynamic amplification factors in cable-stayed structures. Journal of Sound and Vibration 300, 197-216 p.